SPE INSPIRING PLASTICS PROFESSIONALS | POLYMER ENGINEERING AND SCIENCE | WILEY

The effect of the titanium dioxide nanoparticles on the morphology and degradation of polyamide 6 prepared by anionic ring-opening polymerization

Orsolya Viktória Semperger[1] | Zsófia Osváth[2] | Szabolcs Pásztor[2] | András Suplicz[1,3]

[1]Department of Polymer Engineering, Faculty of Mechanical Engineering, Budapest University of Technology and Economics, Budapest, Hungary

[2]Polymer Chemistry Research Group, Institute of Materials and Environmental Chemistry, Research Centre for Natural Sciences, Budapest, Hungary

[3]MTA-BME Lendület Lightweight Polymer Composites Research Group, Budapest, Hungary

Correspondence
András Suplicz, Department of Polymer Engineering, Faculty of Mechanical Engineering, Budapest University of Technology and Economics, Műegyetem rkp. 3., H-1111 Budapest, Hungary.
Email: suplicz@pt.bme.hu

Abstract

Thermoplastic Resin Transfer Molding can be used to produce polyamide 6-based composites from ε-caprolactam by anionic ring-opening polymerization. However, the service life and applicability of these composites are limited because polyamide 6 is sensitive to UV radiation. Therefore, we analyzed the effect of nanosized titanium dioxide on the UV stability of polyamide 6 produced from ε-caprolactam. Despite the very low viscosity of caprolactam, we dispersed nanoparticles homogeneously in it before producing polyamide 6 from it. We have shown that both structural and chemical changes occur in the material under UV exposure. We proved that UV irradiation increases the crystalline fraction of the samples. This is caused by the shortening of the polymer chains. The crystalline fraction increases less with the addition of TiO_2, which shows its UV protective effect. The particles prevent the rays from reaching the inside of the sample, producing a chalking effect on the surface. We analyzed and proved the chemical change in the samples by FTIR and color measurement. Our results showed that surface-treated titanium dioxide was more stable, and the ideal filler content was about 0.6 w/w%, above which photodegradation accelerated. This can be attributed to the photocatalytic activity of the titanium dioxide particles.

KEYWORDS

anionic ring-opening polymerization, chalking, nanosized titanium dioxide, polyamide 6, T-RTM, UV stability, yellowing

1 | INTRODUCTION

Nowadays, the T-RTM (Thermoplastic Resin Transfer Molding) technology is developing more and more dynamically. Several research projects focus on the development of the technology itself, in-mold coating, and the applied raw materials. T-RTM has a number of advantages. Its most important advantage is the impregnation of continuous fiber reinforcements with a low viscosity monomer (ϵ-caprolactam) with a short cycle time at low pressures, producing thermoplastic composites by polymerization. Furthermore, it is possible to create different layer orders within a product, so it can be customized for different loads. Also, the equipment is suitable for mass production due to the short cycle time. The final product is recyclable because of the thermoplastic matrix (polyamide 6), which is a great environmental advantage. Product properties can be modified with fillers. However, the fillers can be filtered out by reinforcement, which can result in inhomogeneities in the product. Therefore, it is necessary to create a surface coating layer through the in-mold coating, to which the fillers can be added. The composite base layer and the surface layer can be produced in one cycle with this technology.[1–9]

Cyclic lactams (amides) are most often produced by anionic ring-opening polymerization.[10–13] The process is popular, not only because it is fast, but also due to its low activation energy and minimal material requirements. The first step in the procedure is initialization.[14–19] In the ring-opening polymerization of lactams, the induction period has slow kinetics, therefore in most cases, activators (mono- or bifunctional) are used to accelerate this.[14–18,20–26] Activators can reduce the temperature required for the reaction and reaction time, and greatly increase conversion.[27,28] During chain growth, the lactam anion activates the lactam monomers in a ring-opening transamidation reaction. The imide anion is formed in the first slow step by a nucleophilic attack of the lactam molecule. Then, after a rapid proton exchange, an imide dimer and a regenerated lactam are obtained. The next step, monomer deprotonation, happens extremely fast. Chain termination reactions are called transfer reactions when additional monomers are available.[29]

The degradation of Nylon 6 is a well-researched[30–53] irreversible process. In this environment, the UV radiation acting as an initiator starts a radical oxidation process in the Nylon that could lead to (depending on the wavelength) chain breaking[35–37] or crosslinking (under 300 nm[38,39]).[36,40,41] These degradation reactions start with the formation of free radicals from carbonyl group precursors.[42,43] A typical degradation sign of Nylons is yellowing, which is caused more by heat than UV radiation. These reactions can start in the methylene group next to the -NH- group, or in the above-mentioned carbonyl groups. The end result is always the same: pyrrol, which is responsible for coloring.[44–48] According to Chien,[49] Tsuji and Seiki[50] free radicals form via oxygen–polymer charge-transfer complexes. Photodegradation in Nylons can manifest itself in different ways, depending on the mechanism of degradation. While chain breaking decreases molecular weight and tensile strength, crosslinking can also increase the stiffness of the material.[30]

There are several ways to prevent the photodegradation of Nylons; with light screeners, UV absorbers, antioxidants, peroxide decomposers, excited-state quenchers or hindered amine light stabilizers (HALS).[30,51–53] Light screeners basically act as passive armor in the material. These inorganic materials (e.g., carbon black or metal oxides, such as TiO_2) limit the penetration of radiation by reflecting or absorbing it. Usually, these also double as pigments or structural strengthening additives.[54–56] All other photo stabilization agents are organic molecules and undergo at least some kind of structural change (e.g., tautomeria or the forming of a coordination complex), but more likely some chemical change while they absorb the UV radiation (UV absorbers) or the radical that was created by the radiation (excited-state quenchers, antioxidants, HALS). It is possible to use more than one kind of photo stabilizer in a product for a combined positive effect.[30]

TiO_2 is a widely used material in the plastic industry as a white pigment, photo-catalyst, and UV-blocker. Due to its low cost, non-toxicity, stability at high temperatures, and under UV exposure, it is gaining in popularity. TiO_2 can improve the UV resistance of polymers, as it is presented in many publications,[57–59] but it can also cause photo-degradation due to its photocatalytic effect.[60] The photocatalysis of TiO_2 is known to generate active oxygen species under ultraviolet exposure. These active oxygen species lead to the degradation reaction by attacking polymer chains and successive chain cleavage.[61] There are several articles in the literature where the properties of polyamide 6 matrices were modified with coated or uncoated TiO_2 particles.[62–65] However, we have not found any comprehensive studies on the UV-blocking effect of

titanium dioxide nanoparticles in the PA6 produced from ε-caprolactam by anionic ring-opening polymerization. This type of polyamide 6 has a different structure (e.g., longer molecular chains, higher crystallinity) than PA6 produced from the melt by injection molding.

Our primary aim is to prepare composite samples by homogeneously dispersing the fillers in the low viscosity raw material. Achieving uniform dispersion is difficult because of the sedimentation and aggregation of the particles. Our further aim is to analyze the effect of neat and surface-coated nanosized titanium dioxide on the photodegradation of polyamide 6, produced by anionic ring-opening polymerization. We studied the structural and chemical changes by examining changes in the crystallinity, color, mass, and surface topology of the samples. In addition to the structural changes caused by UV light, the causes of these changes are also presented.

2 | MATERIALS AND METHODS

2.1 | Materials

The matrix material was produced by anionic ring-opening polymerization from ε-caprolactam (CPL), with the use of an initiator and activator. The initiator was sodium caprolactamate (Brüggolen C10; 1 mol/kg concentration in caprolactam; Brüggemann GmbH and Co. KG, Germany). The activator was bifunctional hexamethylene-1,6-dicarbamoyl-caprolactam (Brüggolen C20P; 2 mol/kg concentration in caprolactam; Brüggemann GmbH and Co. KG, Germany). The ε-caprolactam monomer (AP-NYLON® Caprolactam, L. Brüggemann GmbH and Co. KG, Germany) has lower water content (<100 ppm). The viscosity of the monomer is 4.87 mPa·s at 100°C, its melting point is 71°C, and its boiling point is 270°C. The CPL, the initiator, and the activator were dried at 35°C overnight in a vacuum oven before use. The melting point of C10 is 64°C and that of C20P is 77°C. 94 w/w% CPL, 3 w/w% C10 and 3 w/w% C20P were used to produce polyamide 6.

We used two different rutile types of TiO_2 nanoparticles as inorganic UV stabilizers. The first type was coated with silane (7920SCDL, SkySpring Nanomaterials Inc.) and the second was uncoated (7920DL, SkySpring Nanomaterials Inc.). The average particle size was between 10 and 30 nm in both cases. Different amounts (0, 0.2, 0.4, 0.5, 0.6, 0.8, 1 and 2 w/w%) of TiO_2 were added to the system.

2.2 | Sample preparation

C10 and UV stabilizers and half portions of CPL (mixture A) were poured into a tempered glass sample holder and were dried at 40°C in a vacuum oven for one hour, then deoxygenated by flushing with nitrogen for 5–10 min. The reaction vessel was closed by a septum. C20P and the other half portion of CPL (mixture B) were added in a tempered glass sample holder and were dried and deoxygenated with the same method. These starting materials were heated to 110°C, where all the components melted. After that, mixture B was added to mixture A through a septum with a preheated syringe. After homogenization, the final mixture was heated to the reaction temperature (170°C) in an aluminum mold. After the reaction time (5 min), polymerization was terminated by cooling immediately with room temperature water and dried in a vacuum oven at 40°C until it reached a constant weight.

Samples prepared by anionic ring-opening polymerization have a very long preparation time and most of our tests were time-consuming. Therefore, we selected four formulations (0 w/w% TiO_2; 0.5 w/w% coated and uncoated TiO_2 and 1 w/w% uncoated TiO_2), made three samples using each formulation, and performed repeated tests on these. A total of 23 samples were prepared (15 base samples and 8 repeated samples).

2.3 | Characterization of the samples

2.3.1 | Aging

The 3 mm thick and 15 mm diameter samples were subjected to aging tests for 3 months at 25 RH% and 20°C. The wavelength of the UV tubes was 368 nm, and their average irradiance was 3900 μW/cm² (39 W/m²) on the surface of the samples. The distance of the samples from the UV fluorescent tubes was 40 mm (Figure 1). Prior to the start of the experiment, the specimens were dried at 80°C for 8 h. The samples were directly below the UV tube, therefore the angle of the rays was 90°. During the study, radiation was constant.

FIGURE 1 Measurement arrangement

2.3.2 | Measurement methods

The dispersion of TiO₂ was analyzed by EDS (Energy Dispersive Spectroscopy) with a JEOL JSM 6380LA electron microscope. The surface of the specimens was coated with an Au/Pd alloy prior to observation as this eliminates undesirable electrostatic charging.

Crystallinity was determined from the average of three samples with a TA DSC Q2000 (TA Instruments, USA) apparatus both before and after aging. 3–5 mg samples were cut off from the surface of the specimens and placed in an aluminum lid. The measurement procedure consisted of three stages: heating–cooling–heating between 20°C and 250°C. The heating and cooling rate was 10°C/min, in a nitrogen atmosphere. The crystallinity of the samples was determined from the endothermic peaks of DSC (Differential Scanning Calorimetry) curves with the following Equation (1):

$$x = \frac{\Delta H_m - \Delta H_{cc}}{\Delta H_{kr} \cdot (1 - \alpha)} \cdot 100 \, [\%], \tag{1}$$

where x [%] is the crystallinity of the samples, ΔH_m [J/g] is the melting enthalpy, ΔH_{kr} [J/g] is the melting enthalpy of a theoretically fully crystalline polymer, ΔH_{cc} [J/g] is the enthalpy of cold crystallization and α [w/w%] is the filler fraction of the samples. In the case of polyamide 6, $\Delta H_{kr} = 188$ J/g.[66]

The weights of the samples were measured with a Steinberg SBS-LW-2000A scale after every 3 days of UV exposure. The mass loss of the samples was calculated from the measured weights.

The color of the samples was determined with a Color-Guide Sphere apparatus (BYK-Gardner, Germany) after every 3 days. The color was measured in three different positions on the surface and then the results were averaged. Of the CIE Lab color coordinates, we examined the b* (blue/yellow) parameter as a function of time and filler content to characterize the yellowing of the samples.

The surface topology of the samples was characterized by an AFM (Atomic Force Microscope) (Nanosurf FlexAFM 5, Nanosurf AG, Liestal, Switzerland) in tapping mode in the air at room temperature. A single-beam silicon cantilever was used for the analysis (TAP 190Al-G, Budget Sensors, Innovative Solutions Bulgaria Ltd., Sofia, Bulgaria).

The chemical structure of polyamide samples was analyzed with an ATR-FTIR (Fourier-Transform Infrared Spectroscopy) apparatus (Bruker Tensor II, Bruker Optics Inc., Billerica, MA). Its wavelength range is from 4000 to 400 cm^{-1}. Sixteen scans were performed and averaged on each sample. The results were evaluated with the OPUS 8.2 software.

3 | RESULTS AND DISCUSSION

3.1 | Evaluation of TiO₂ dispersion

Homogeneous filler dispersion is critical in maximizing the UV resistance of polymers. Therefore, we investigated the distribution of titanium dioxide particles in the samples by EDS. Figure 2 shows an example of the results. The red dots indicate the location of the detected Ti atoms when filler content was 0.2 w/w% and 1 w/w%. Despite the small shear applied, both surface-treated and untreated TiO₂ particles were homogeneously distributed in the matrix material—no larger aggregates were found. As the particles were distributed homogeneously, the changes experienced in further studies were caused by the type and amount of filler and not the unevenness of dispersion.

3.2 | DSC analysis of the samples

Figures 3 and 4 present the crystallinity of the TiO₂-filled samples before and after aging. The results show that the applied nanosized TiO₂ increased the crystallinity of the samples in every case. 2 w/w% uncoated and coated TiO₂ increased the crystalline proportion by 46% and 21%, respectively. After 90 days of UV irradiation, the crystallinity of the polyamides increased further, compared to the initial values. In both cases, these differences decreased as filler concentration was increased in the investigated range. The largest change occurred in the case of unfilled specimens (~43%). When filler concentration was 2 w/w%, UV radiation-induced a change in crystallinity of only 8.1% (uncoated TiO₂) and 22.7% (coated TiO₂). The results indicate that the addition of nanoscale TiO₂ can be an effective method to reduce the negative effects of UV radiation, because the structure of TiO₂-filled polyamide is more stable.

A two-sample t-test was used to analyze the significant difference in crystallinity of the repeated experiments before and after UV treatment. The analysis shows that the p-value at the 0.05 significance level is less than 0.04 in all cases. In addition, we performed a two-sample t-test to determine whether there was a significant difference in the crystalline fraction of all samples before and after UV treatment. At a significance level of 0.05, $p = .0006$ was found for untreated TiO₂ and $p = .000013$ for surface-treated particles. These results indicate that the difference is significant in both cases.

We compared the first heating stages of the DSC curves of the samples before and after aging. Figure 5 clearly shows that the crystals started melting earlier after irradiation. This is due to the shortening of polymer molecular

FIGURE 2 EDS analysis of the nanocomposites filled by 0.2 w/w% and 1 w/w% TiO$_2$ (red marks indicate the detected Ti atoms)
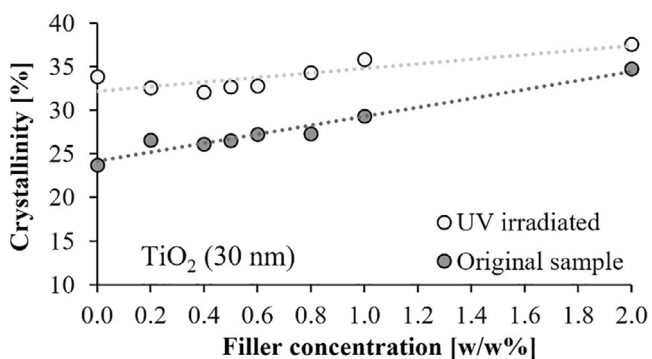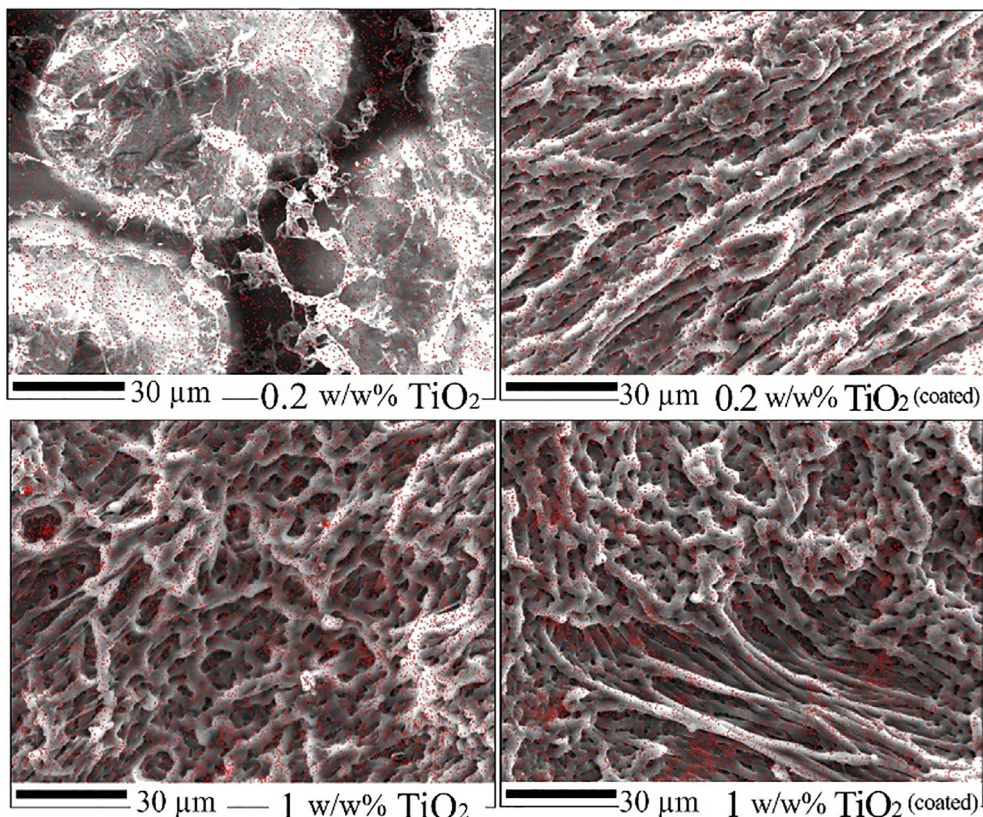

FIGURE 3 Changes in the crystallinity of samples with uncoated TiO$_2$
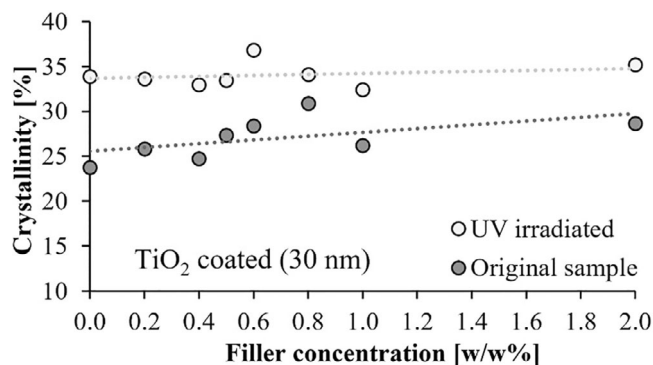

FIGURE 4 Changes in the crystallinity of samples with coated TiO$_2$

chains, caused directly by the UV rays or the photocatalytic effect of TiO$_2$ nanoparticles. These shorter chains have more mobility, therefore the smaller crystals are capable of post-crystallization.

Polymers containing covalent bonds consist of long molecular chains. The length, complexity, and orientation of molecular chains can be varied, which influences their mechanical and morphological properties. Polyamides are characterized by the amide bond (-CONH-). The different chemical groups can absorb different amounts of energy. Long-chain molecules can break apart and create shorter molecules because of high-energy photons.

The absorption of UV photons can help bring electrons to higher energy levels and it can separate chemical bonds. As a result, the mechanical properties and the appearance of the polymer may change. Furthermore, by-products may be released and leave the surface of the polymer due to chain breaking.[65] In addition, the breakdown of chemical bonds by UV radiation produces free radicals. These free radicals are highly reactive, so they can react with the oxygen or water in their environment. This damages the polymer (oxidation and hydrolysis).

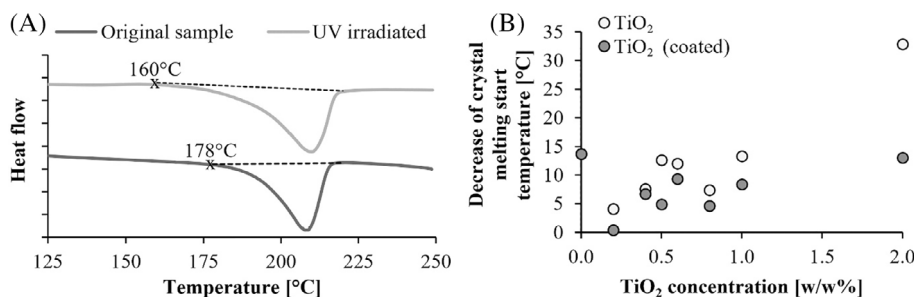The other effect that can cause chain breaking in polymer/TiO$_2$ nanocomposites is the photocatalytic
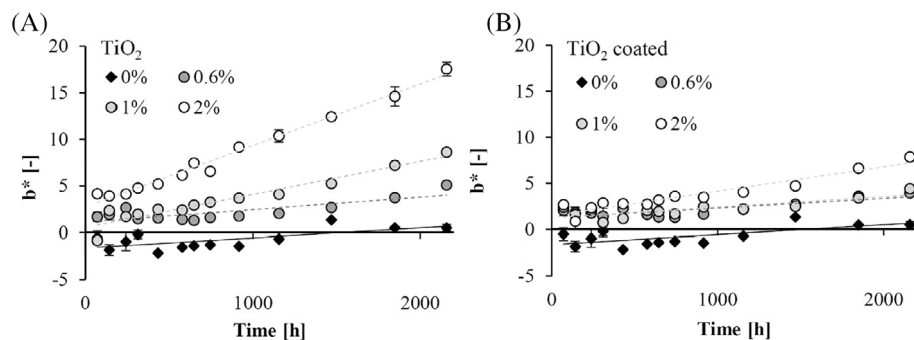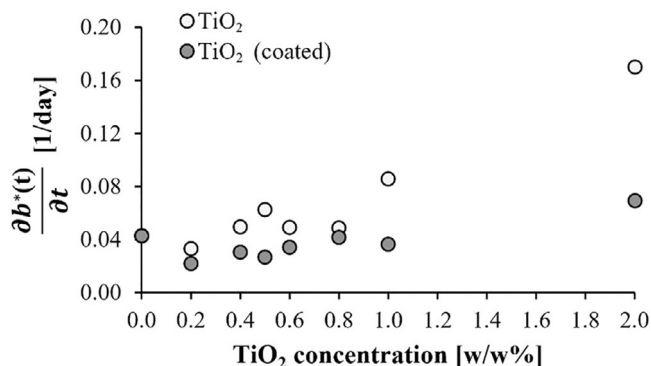
activity of titanium dioxide. TiO_2 particles can absorb energy from UV irradiation. Thanks to this energy, the electron (e^-) in TiO_2 can jump to the conduction band, leaving a positive hole (h^+) in the valence band. The electrons can easily react with O_2, and the holes in the conduction band with H_2O. These reactions result in O_2^- and OH^- radicals with high chemical activity, which causes a degradation reaction—the radicals attack polymer chains and accelerate chain cleavage.[60]

3.3 | Yellowing of the samples

The yellowing of the specimens can be characterized with b* of the CIE Lab color coordinates. We found that b* changed nearly linearly with aging time in the analyzed period (Figure 6).

Therefore, we calculated the derivative of b* ($\partial b^*/\partial t$), which shows the rate of color change. Figure 7 shows the time derivative of b* as a function of filler content. When a low amount of nanosized titanium-dioxide was added to the PA6, the yellowing rate slowed down. It means that UV resistance can be improved if the amount of uncoated or coated TiO_2 is increased up to 0.4 w/w% or 0.8 w/w%, respectively. Above these concentrations, discoloration exceeds that of the unfilled material. One possible explanation is that the UV filtering effect of nanosized TiO_2 can no longer compensate for its photocatalytic effect. Another reason could be that the increased filler content forces the high-energy UV rays closer to the surface, where they have a more concentrated effect, increasing degradation. Also, yellowing was minimal in samples with coated TiO_2, while it was significant in specimens filled with uncoated TiO_2.

3.4 | UV radiation-induced mass change

Figure 8 shows the change of sample mass during the whole aging period as a function of filler content. Weight does not show a significant change up to 0.6 w/w% TiO_2 concentration. 1 w/w% uncoated TiO_2 causes a significant mass loss (1.8%), and 2 w/w% uncoated TiO_2 results in a total mass loss of 8%. Mass loss was lower when coated TiO_2 was added. From these results and from the repeated experiments, we concluded that the highest filler content should be chosen where the difference between the initial and final weight does not increase

significantly yet (∼0.4–0.6 w/w%). Furthermore, coated TiO$_2$ was more stable than uncoated TiO$_2$.

An explanation for the mass change can be chalking. When polymers are exposed to UV light, a thin layer of loosely adherent particles is generated on the surface. During the process, the organic molecules erode and the fillers are left on the surface as a chalky layer. Another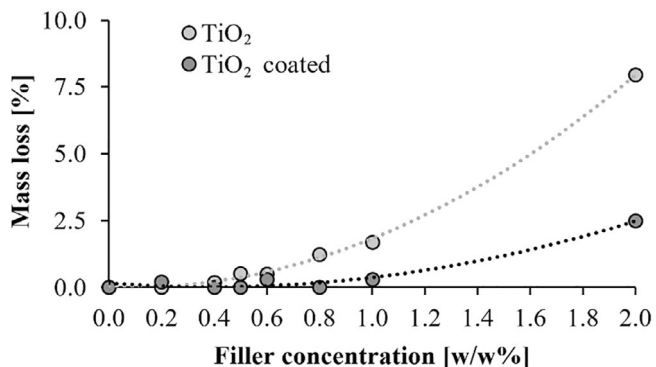 reason for the mass change can be the vaporization of low molecular weight and highly volatile products from the sample.[67,68] From the degraded and depolymerized chains, low molecular weight oligomers and polymers can separate, diffuse toward the surface, and evaporate from the material. If the UV light source also generates heat, the evaporation rate increases.

To analyze chalking, we examined the surface of the samples by AFM. The results are shown in Figures 9 and 10, for uncoated and coated TiO$_2$, respectively. The microscopic images show that the surface topology changes slightly with aging. Surface roughness decreased, and the surface of the samples became smoother, probably due to the effect of heat. It is more pronounced when the concentration of nanosized TiO$_2$ is increased. The images prove chalking and chalking causes mass change.

FIGURE 8 Mass loss after 90 days of aging as a function of filler concentration

3.5 | FTIR analysis

Since we wanted to see if there was also a change in the chemical structure, as indicated by the yellowing of the sample, we carried out FTIR studies. Studies in the literature indicated which peaks to examine for changes, and

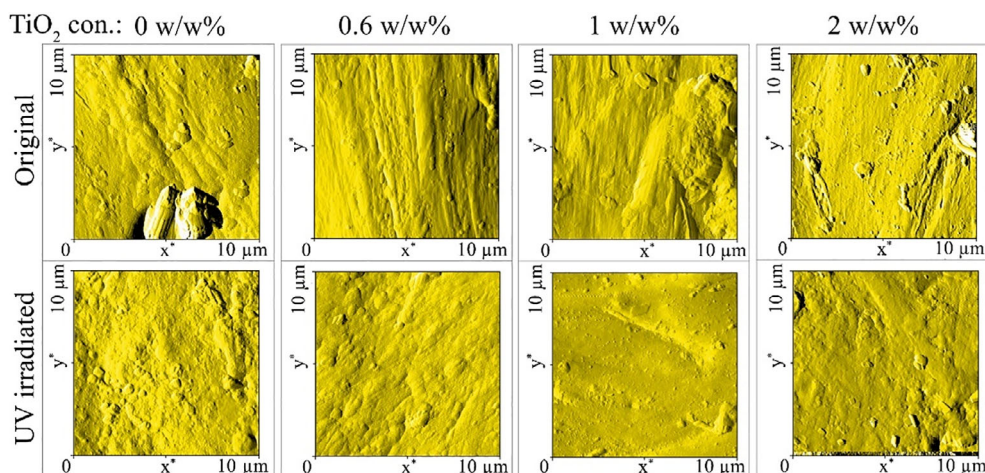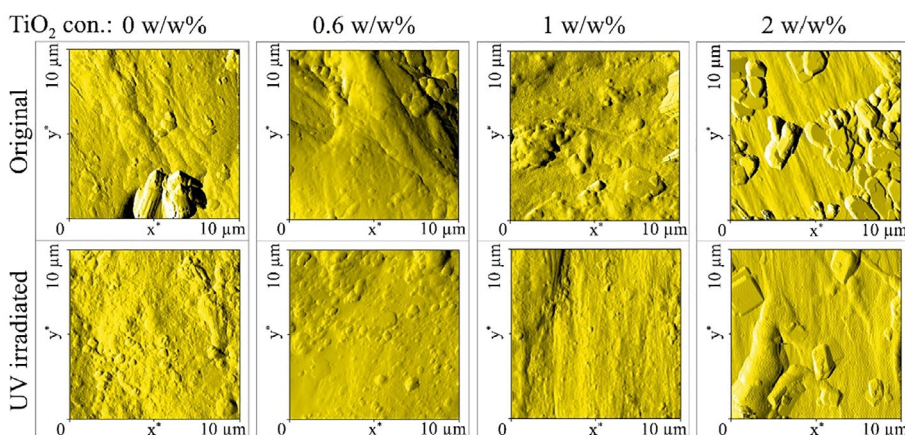**FIGURE 9** AFM images of the uncoated, nanosized TiO$_2$-filled samples before and after aging

FIGURE 10 AFM images of the coated, nanosized TiO$_2$-filled samples before and after aging
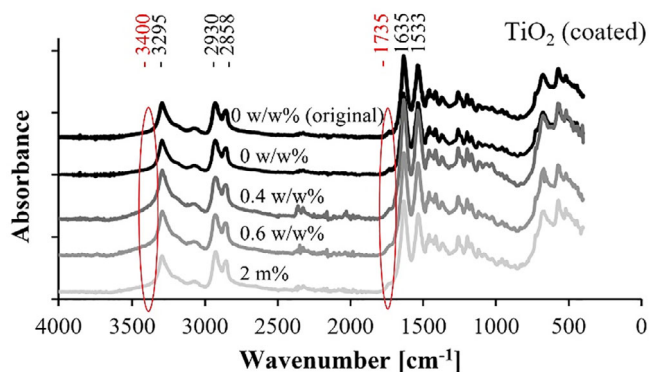
FIGURE 11 Infrared spectra of coated TiO₂-filled samples after UV irradiation
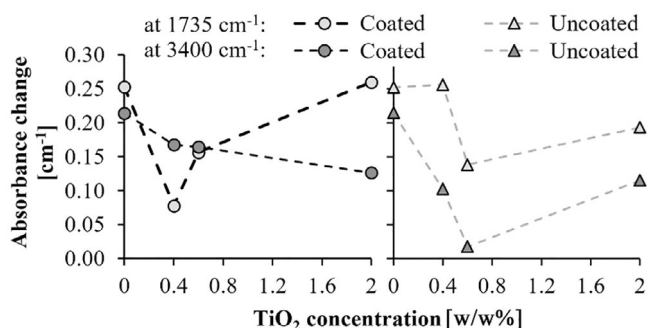

FIGURE 12 Absorbance increment of the samples at 1735 and 3400 cm⁻¹ due to UV irradiation

we observed these peaks, where changes were expected. The IR spectra of the UV-exposed samples is shown in Figure 11. The IR spectra show a peak around 3295 cm⁻¹, which is assigned to the N—H stretching of hydrogen-bonded N—H groups. The next two characteristic peaks, around 2930 and 2854 cm⁻¹ show the asymmetric (in-phase) and symmetric (out of phase) C—H stretching vibrations. The bands located around 1635 and 1533 cm⁻¹ can be attributed to C=O (mode I of amide) and N—H and C—N combination (amide II stretch) vibration, respectively.[69–71] Similarly to Roger et al.,[72] we observed the change of absorption bands around 3400 and 1735 cm⁻¹, which could be a sign of photooxidation. The increase in the absorption bands at 1735 cm⁻¹ can be attributed to the formation of imide groups, and the unstructured shoulder in the N—H absorption band around 3400 cm⁻¹ is attributed to N-l-hydroxylated groups when polyamide samples are photodegraded with long-wavelength UV radiation (>340 nm).[70]

The absorbance difference at 3400 and 1735 cm⁻¹ before and after 90 days of UV exposure is presented in Figure 12. Based on the yellowing analysis, the optimum TiO₂ concentration is 0.4–0.6 w/w% because it can

minimize photodegradation. At higher concentrations, the absorbance difference increases, due to accelerated degradation.

4 | CONCLUSION

We prepared polyamide 6 by anionic ring-opening polymerization from ε-caprolactam and filled it with nanosized TiO₂. Uncoated and coated TiO₂ were added in the 0–2 w/w% concentration range. The fillers were dispersed uniformly despite the low viscosity of the raw material. This was proved by EDS. The composite samples were exposed to UV irradiation for 90 days. We studied the effects of UV exposure on the chemical composition and structure of the samples and proved by DSC that UV irradiation increased their crystalline fraction. The crystalline fraction increased due to the breakup and shortening of the polymer chains. The shorter chains are more mobile, so post-crystallization occurs more easily. Chain shortening was confirmed by the melting of the crystals at lower temperatures after UV irradiation. The difference in crystallinity between the initial and irradiated samples decreased as filler concentration was increased. This is due to the UV-protective effect of TiO₂ and because the particles decrease chain mobility. We also proved that chalking occurs in the composite samples, and it increases with filler concentration. This is because the TiO₂ particles reflect UV rays, concentrating their effect near the surface. The polyamide samples also showed strong yellowing after UV irradiation. Up to 0.6 w/w% TiO₂ concentration, yellowing was reduced. In the case of both coated and uncoated TiO₂, there was a significant increase in yellowing above a filler content of 0.6 w/w%. We performed FTIR to analyze the chemical changes. Studies in the literature indicated peaks to examine for changes - the change of absorption bands was at 3400 and 1735 cm⁻¹. The FTIR analysis showed that the optimum TiO₂ concentration is 0.4–0.6 w/w%, because this concentration of TiO₂ can minimize photodegradation. At higher concentrations, the absorbance difference increases, which can be attributed to accelerated degradation.

In summary, the UV stability of polyamide 6 can be improved by the addition of up to 0.6 w/w% of nanosized titanium dioxide, above which significant surface degradation occurs under UV irradiation. This is because the reflective effect of nanoscale TiO₂ can no longer compensate for its photocatalytic effect. Another reason is that the increased filler content forces the high-energy UV rays closer to the surface, where they are more concentrated, enhancing degradation. We also showed that surface-treated TiO₂ made PA6 samples more stable than untreated TiO₂.

DATA AVAILABILITY STATEMENT

The data that support the findings of this study are available from the corresponding author upon reasonable request.

ORCID

Orsolya Viktória Semperger https://orcid.org/0000-0003-1736-9624
András Suplicz https://orcid.org/0000-0002-0304-7491

REFERENCES

[1] M. Thomassey, B. P. Revol, F. Ruch, J. Schell, M. Bouquey, *Univers J. Mater. Sci.* **2017**, *5*(1), 15.

[2] C. C. Höhne, R. Wendel, B. Käbisch, T. Anders, F. Henning, E. Kroke, *Fire Mater.* **2016**, *41*(4), 291.

[3] L. Jungwoo, W. L. Jun Woo, K. Minkook, *Polym. Compos.* **2019**, *41*(4), 1190.

[4] J. Herzog, R. Wendel, P. G. Weidler, M. Wilhelm, P. Rosenberg, F. Henning, *J. Compos. Sci.* **2021**, *5*(1), 12.

[5] L. Lewerdomski, C. Schütz, *Lightweight Des Worldwide* **2019**, *12*(5), 38.

[6] N. Zaldua, J. Maiz, A. de la Calle, S. García-Arrieta, C. Elizetxea, I. Harismendy, A. Tercjak, A. J. Müller, *Polymer* **2019**, *11*(10), 1680.

[7] R. Wendel, B. Thoma, F. Henning. 33rd Int. Conf. Polym. Process. Soc., Cancun, (**2017**)

[8] O. V. Semperger, A. Suplicz, *Materials* **2020**, *13*, 4.

[9] K. S. Boparai, R. Singh, F. Fabbrocino, F. Fraternali, *Compos. Part B* **2016**, *106*, 42.

[10] S. Russo, E. Casazza, *Polym. Sci. A Compos. Ref.* **2012**, *4*, 331.

[11] Z. Osváth, A. Szőke, S. Pásztor, L. B. Závoczki, G. Szarka, B. Iván, *Acad. J. Polym. Sci.* **2020**, *4*(1), 118.

[12] K. Hashimoto, *Prog. Polym. Sci.* **2000**, *25*(10), 1411.

[13] L. Song, X. Wang, P. Xie, Y. Ding, K. Dang, W. Yang, *Polym. Eng. Sci.* **2021**, *61*, 1662.

[14] D. Tunc, H. Bouchekif, B. Améduri, C. Jérôme, P. Desbois, P. Lecomte, S. Carlotti, *Eur. Polym. J.* **2015**, *71*, 575.

[15] N. Barhoumi, A. Maazouz, M. Jaziri, R. Abdelhedi, *Expr. Polym. Lett.* **2013**, *7*(1), 76.

[16] G. Evans, P. Desbois, A. Lesser, *J. Appl. Polym. Sci.* **2018**, *135*, 46823.

[17] N. Zhu, H. Gong, W. Han, W. Zeng, H. Wang, Z. Fang, X. Li, K. Zhang, Z. Li, K. Guo, *Chin. Chem. Lett.* **2015**, *26*(11), 1389.

[18] A. Maazouz, K. Lamnawar, M. Dkier, *Compos. Part A: Appl. Sci. Manuf.* **2018**, *107*, 235.

[19] C. Vicard, O. Almeida, A. Cantarel, G. Bernhart, *Polymer* **2017**, *132*, 88.

[20] F. Oliveira, N. Dencheva, P. Martins, S. Lanceros-Méndez, Z. Denchev, *Expr. Polym. Lett.* **2016**, *10*(2), 160.

[21] C. Breda, N. Dencheva, S. Lanceros-Mendez, Z. Denchev, *J. Mater. Sci.* **2016**, *51*(23), 10534.

[22] K. Udipi, R. S. Davé, R. Kruse, L. Stebbins, *Polymer* **1997**, *38*(4), 927.

[23] G. Rusu, K. Ueda, E. Rusu, M. Rusu, *Polymer* **2001**, *42*(13), 5669.

[24] D. Crespy, K. Landfester, *Macromolecules* **2005**, *38*(16), 68826887.

[25] J. Budin, J. Brozek, J. Roda, *Polymer* **2006**, *47*(1), 140.

[26] J. Budin, J. Roda, J. Brozek, J. Krir, *Macromol. Symp.* **2006**, *240*(1), 78.

[27] S. Russo, S. Maniscalo, L. Ricco, *Polym. Adv. Technol.* **2015**, *26*(7), 851.

[28] Z. Osváth, A. Szőke, S. Pásztor, L. B. Závoczki, G. Szarka, B. Iván, *Processes* **2020**, *8*(7), 856.

[29] O. Nuyken, S. Pask, *Polymer* **2013**, *5*(2), 361.

[30] P. N. Thanki, R. P. Singh, *J. Macromol. Sci. Part C* **1998**, *38*(4), 595.

[31] N. S. Allen, M. J. Harrison, G. W. Follows, V. Matthews, *Polym. Degrad. Stab.* **1987**, *19*(1), 77.

[32] N. S. Allen, M. J. Harrison, G. W. Follows, *Polym. Degrad. Stab.* **1988**, *21*(3), 251.

[33] N. S. Allen, M. J. Harrison, M. Ledward, G. W. Follows, *Polym. Degrad. Stab.* **1989**, *23*(2), 165.

[34] Y. W. Mai, D. R. Head, B. Cotterell, *J. Mater. Sci.* **1980**, *15*, 3057.

[35] H. M. Heuvel, K. C. J. Lind, *J. Polym. Sci. Part A-2: Polym. Phys.* **1970**, *8*(3), 401.

[36] R. F. Moore, *Polymer* **1963**, *4*, 493.

[37] C. V. Stephenson, J. C. Lacey, W. S. Wilcox, *J. Polym. Sci.* **1961**, *55*(162), 477.

[38] B. S. Stowe, R. E. Fornes, R. D. Gilbert, *Polym.-Plast. Technol. Eng.* **1974**, *3*(2), 159.

[39] S. Yano, M. J. Murayama, *Appl. Polym. Sci.* **1980**, *25*(3), 433.

[40] B. Ranby, J. F. Rabek, in *Photodegradation, Photo-oxidation and Photostabilization of Polymers* (Ed: E. Pearce), Wiley, New York **1975**, p. 236.

[41] C. V. Stephenson, B. C. Moses, R. E. Burks, W. C. Coburn, W. S. Wilcox, *J. Polym. Sci.* **1961**, *55*(162), 465.

[42] J. G. Kalvert, J. N. Pitts, in *Photochemistry* (Ed: G. Quinkert), Wiley, New York **1966**, p. 84.

[43] H. J. Heller, *Eur. Polym. J.* **1969**, *5*, 105.

[44] P. Rochas, J. C. Martin, *Bull. Inst. Text France* **1959**, *83*, 41.

[45] E. H. Boasson, B. Kamerbeck, A. Algera, G. H. Kores, *Rec. Trav.Chim. Pays Bas* **1962**, *81*(7), 624.

[46] B. Marek, E. Lerch, *J. Soc. Dye. Colour.* **1965**, *81*(11), 481.

[47] N. S. Allen, J. F. McKeller, G. O. Phillips, *J. Polym. Sci. Polym. Chem. Ed.* **1974**, *12*(6), 1233.

[48] N. S. Allen, J. F. McKeller, G. O. Phillips, *J. Polym. Sci. Polym. Chem. Ed.* **1974**, *12*(11), 2623.

[49] J. C. W. Chien, *J. Phys. Chem.* **1965**, *69*(12), 4317.

[50] K. Tsuji, T. Seiki, *J. Polym. Sci., Part A: Polym. Chem.* **1971**, *9*(10), 3063.

[51] H. Zweifel, R. D. Maier, M. Schiller, in *Plastics Additives Handbook*, 6th ed. (Ed: H. Zweifel), Hanser, Munich **2009**, p. 1248.

[52] G. Pieter, in *Photochemistry and Photophysics of Polymeric Materials* (Ed: N. S. Allen), Wiley, New York **2010**, p. 709.

[53] P. Cerruti, M. Lavorgna, C. Carfagna, L. Nicolais, *Polymer* **2005**, *46*(13), 4571.

[54] F. Fasahat, R. Dastjerdi, M. R. M. Mojtahedi, P. Hoseini, *Wear* **2015**, *322-323*, 117.

[55] H. Nagasawa, J. Xu, M. Kanezashi, T. Tsuru, *Mater. Lett.* **2018**, *228*, 479.

[56] C. Li, Z. Li, X. Ren, *Colloids Surf. A Physicochem. Eng. Asp.* **2019**, *577*, 695.

[57] Y. Cao, P. Xu, W. Yang, X. Zhu, W. Dong, M. Chen, M. Du, T. Liu, P. J. Lemstra, P. Ma, *Compos. Part B* **2021**, *205*, 1.

[58] L. C. Mohr, A. P. Capelezzo, C. R. D. M. Baretta, M. A. P. M. Martins, M. A. Fiori, J. M. M. Mello, *Polym. Test.* **2019**, *77*, 1.

[59] M. Decol, W. M. Pachekoski, D. Becker, *Polym. Eng. Sci.* **2020**, *60*, 2439.

[60] N. Nakayama, T. Hayashi, *Polym. Degrad. Stab.* **2007**, *92*, 1255.

[61] S. H. Kim, S.-Y. Kwak, T. Suzuki, *Polymer* **2006**, *47*, 3005.

[62] G. Rusu, E. Rusu, *Int. J. Polym. Anal. Charact.* **2011**, *16*(8), 651.

[63] G. Rusu, E. Rusu, *Polym. Compos.* **2012**, *9*, 1557.

[64] Y. Yu-ting, Y. Chun-wang, *J. Mater. Sci.* **2019**, *54*, 9456.

[65] R. Soundararajan, N. Jayasuriya, R. G. Girish Vishnu, B. G. Prassad, C. Pradeep, *Mater. Today: Proc.* **2019**, *18*, 2394.

[66] J. E. Mark, in *The Polymer Data Handbook* (Ed: J. E. Mark), Oxford University Press, Oxford **1999**, p. 1264.

[67] V. C. Malshe, G. Waghoo, *Prog. Org. Coat.* **2004**, *51*(3), 172.

[68] T. Lu, E. Solis-Ramos, Y. Yi, M. Kumosa, *Polym. Degrad. Stab.* **2018**, *154*(4), 203.

[69] F. Mindivan, *Materials* **2016**, *11*, 56.

[70] J. C. Farias-Aguilar, M. J. Ramírez-Moreno, L. Téllez-Jurado, H. Balmori-Ramírez, *Mater. Lett.* **2014**, *136*, 388.

[71] K. Liu, Y. Li, L. Tao, R. Xiao, *RSC Adv.* **2018**, *8*(17), 9261.

[72] A. Roger, D. Sallet, J. Lemaire, *Macromolecules* **1986**, *19*(3), 579.